



A measurement of forward-backward charge asymmetry in top pair production

The DØ Collaboration
URL <http://www-d0.fnal.gov>

We present a first measurement of the integrated forward-backward charge asymmetry in top-antitop quark pair ($t\bar{t}$) production in proton-antiproton collisions at $\sqrt{s} = 1.96$ TeV. The measurement is performed in the lepton + jets final state using events selected with a neural net b -tagger and reconstructed using a kinematic fitter. Using a 0.9 fb^{-1} dataset collected by the DØ experiment at the Fermilab Tevatron collider, we measure an integrated asymmetry, uncorrected for reconstruction effects, of $(12 \pm 8 \text{ (stat)} \pm 1 \text{ (syst)}) \%$, for a specific region of phase space. We provide functional forms that allow the comparison of any model to the measured asymmetry. We use the measurement to place limits on $t\bar{t}$ production via a Z' resonance.

Preliminary Results for Summer 2007 Conferences

PACS numbers: 12.38.Qk, 12.60.-i, 13.85.-t, 13.87.Ce

I. INTRODUCTION

At lowest order in quantum chromodynamics (QCD), the standard model predicts that top quark pair production in $p\bar{p}$ interaction is charge symmetric. But this symmetry is accidental, as the initial $p\bar{p}$ state is not an eigenstate of the charge conjugation operator. Next-to-leading order (NLO) calculations predict forward-backward asymmetries of 5-10% [1, 2], but recent next-to-next-to-leading order (NNLO) calculations predict large corrections [3]. This asymmetry arises mainly from interference between contributions symmetric and antisymmetric under the exchange $t \rightarrow \bar{t}$ [1], and depends strongly on the region of phase space being probed, and, in particular, on any extra jet production [2]. The low asymmetries expected in the standard model makes this a sensitive probe for new physics.

The top charge asymmetry is most suited to measurement at the Tevatron, as in proton-antiproton collisions it can be directly observed as a forward-backward asymmetry, and contributions from charge-symmetric gluon-gluon fusion processes are small. The signed difference between the reconstructed rapidities of the t and \bar{t} , $\Delta y \equiv y_t - y_{\bar{t}}$, measures the asymmetry in $t\bar{t}$ production. We define forward and backward events by the sign of Δy and then define the asymmetry to be:

$$A_{fb} = \frac{N^{\Delta y > 0} - N^{\Delta y < 0}}{N^{\Delta y > 0} + N^{\Delta y < 0}}. \quad (1)$$

This note describes a first measurement of the integrated charge asymmetry in $t\bar{t}$ production in proton-antiproton collisions at $\sqrt{s} = 1.96$ TeV, using 0.9 fb^{-1} of data. The data were collected from 2002 to 2005 using the D0 detector [4] with triggers that required a jet and an electron or muon. The lepton+jets decay mode of the $t\bar{t}$ quark pair, where one of the two W bosons from the top or antitop quarks decays into hadronic jets and the other decays to leptons, is particularly suitable for this measurement. The lepton+jets channel combines a large branching fraction ($\approx 34\%$) with high purity of signal, as a consequence of requiring an isolated electron or muon of large transverse momentum (p_T). This channel offers accurate reconstruction of the $t\bar{t}$ directions in the collision rest frame, and the charge of the electron or muon provides an excellent tag for the t or \bar{t} quark.

II. THEORY AND STRATEGY

The dependence of the asymmetry on the region of phase space, as calculated by the MC@NLO event generator [5], is demonstrated in Fig. 1. The large dependence on the 4th highest jet p_T is not considered in the calculations of Ref. [1–3], as they do not decay the top quarks, and consider acceptance only for jets from additional radiation.

We conclude that the acceptance can strongly shape the asymmetry, mostly through the criteria imposed on jet p_T . In order to facilitate comparisons with theoretical calculations, the analysis is therefore designed to have an acceptance which can be simply described. This is done by limiting the event selection to either: (i) simple selections on object directions and momenta that can be described at the particle level, or (ii) criteria with high signal efficiency, so that their impact on the region of acceptance is negligible. In addition, the observable quantity and fitting procedure were chosen to assure that all selected events have the same weight in determining the asymmetry.

The measurement is not corrected for acceptance and reconstruction effects. Instead, a prescription is given which allows one to describe the acceptance at the particle level. The reconstruction effects (misreconstruction of the sign of Δy) can be accounted for by folding the resulting asymmetry as a function of the generated Δy :

$$A_{fb}^{pred} = \int_0^\infty A_{fb}(|\Delta y_{\text{gen}}|) \mathcal{D}(|\Delta y_{\text{gen}}|) f(|\Delta y_{\text{gen}}|) d|\Delta y_{\text{gen}}|, \quad (2)$$

where \mathcal{D} is the "geometric dilution" detailed later, and f is the probability density predicted for $|\Delta y|$. With this procedure the MC@NLO prediction for the uncorrected top asymmetry is:

$$A_{fb}^{pred} = (0.8 \pm 0.2 \text{ (stat)} \pm 1.0 \text{ (accept)}) \%, \quad (3)$$

with dilution uncertainties below 0.1%. This prediction is an order of magnitude smaller than that of Ref. [1, 2]. The difference is due to the jet acceptance cuts, the dilution, and to the almost perfect cancellation of $t\bar{t}$ and $t\bar{t}j$ contributions to A_{fb} within our acceptance. A_{fb}

III. SELECTION AND RECONSTRUCTION

We select events with at least four jets, reconstructed using a cone algorithm [6] with a angular radius $\mathcal{R} = 0.5$ (in rapidity and azimuthal angle, ϕ) to cluster energy deposits in the calorimeter. All jets have $p_T > 20 \text{ GeV}$ and

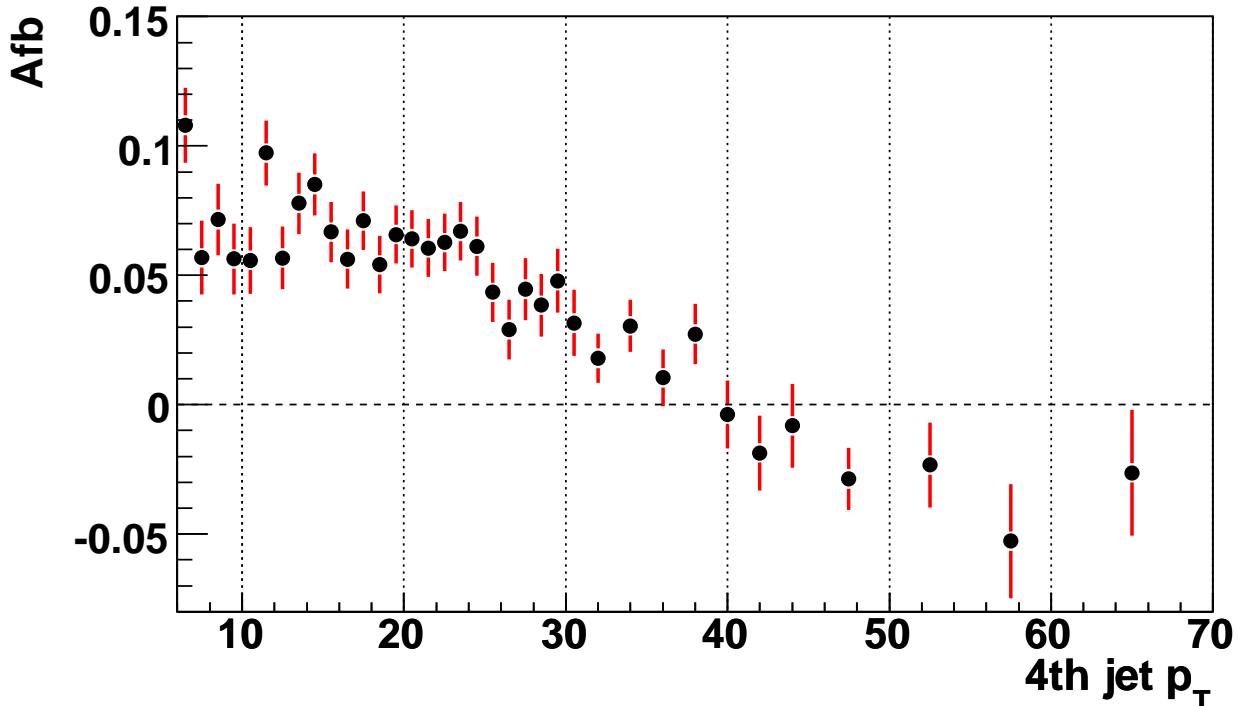


FIG. 1: Forward-backward top charge asymmetry from MC@NLO as a function of the 4th highest jet p_T . The only additional selection requirement is that of semi-leptonic $t\bar{t}$ decay.

pseudorapidity (relative to the center of the detector) $|\eta| < 2.5$, and the leading jet has $p_T > 35$ GeV. Events are required to have missing transverse energy, \cancel{E}_T , above 15 GeV and exactly one isolated electron with $p_T > 15$ GeV and $|\eta| < 1.1$ or one isolated muon with $p_T > 18$ GeV and $|\eta| < 2.0$. More details on lepton identification and trigger requirements are given in Ref. [7]. Events where lepton momentum is misreconstructed are suppressed by requiring that the direction of the \cancel{E}_T is not aligned or antialigned in azimuth with the lepton. The \cancel{E}_T requirements used are $> 95\%$ efficient for signal. To enhance the signal content of the selection, at least one of the jets is required to be identified as originating from long-lived b hadrons by a neural network b -jet tagging algorithm [8]. The variables used to identify such jets rely on the presence and characteristics of a secondary vertex and tracks with high impact parameters inside the jet. The b -tagging requirement used is 84% efficient for signal.

The top pair is reconstructed from its decays using a kinematic fitter [9]. The fitter varies the kinematics of the detected objects within their resolutions, and minimizes a χ^2 statistic with the constraints that both W boson masses are exactly 80.4 GeV and both top quark masses are exactly 175 GeV. In each event the b -tagged jet with the largest p_T , i.e. the hardest, and the three hardest remaining jets are considered in the fit. The b -tagging information is used to reduce the number of jet-parton assignments considered in the kinematic fitter. Only events in which the kinematic fit converges are used, and for each event only the solution with the lowest χ^2 is retained. The kinematic fitter converges for over 90% of $t\bar{t}$ events.

IV. ACCEPTANCE

The jet p_T selection criteria strongly affect the observed asymmetry (see Fig. 1), and these effects must be applied to a model's asymmetry before comparing with our data. Fortunately, the acceptance effects can be approximated by simple cuts on particle level kinematics without changing the asymmetry by more than 2% (absolute). This was verified using several simulated samples with generated asymmetries, with particle jets clustered by the PXCONE algorithm [10] using the “E” scheme and $\mathcal{R} = 0.5$. The simple particle-jet cuts are $p_T > 21$ GeV and $|\eta| < 2.5$, with the additional requirement on the leading particle jet $p_T > 35$ GeV and the lepton requirements detailed above, where the uncertainties are due to uncertainties on the jet energy calibration. The effect of all additional criteria on the asymmetry is negligible. In this note we also use a fuller description based on efficiencies factorized in p_T and η , that is accurate to within 1% (absolute).

TABLE I: Dilution Parameters.

Variation	c_1	c_2	c_3	c_4	c_5
Nominal	2.570	4.838	4.977	2.479	0.4674
+1 σ systematic	2.748	-5.038	4.866	-2.253	0.3969
-1 σ systematic	2.327	-3.926	3.462	-1.468	0.2391

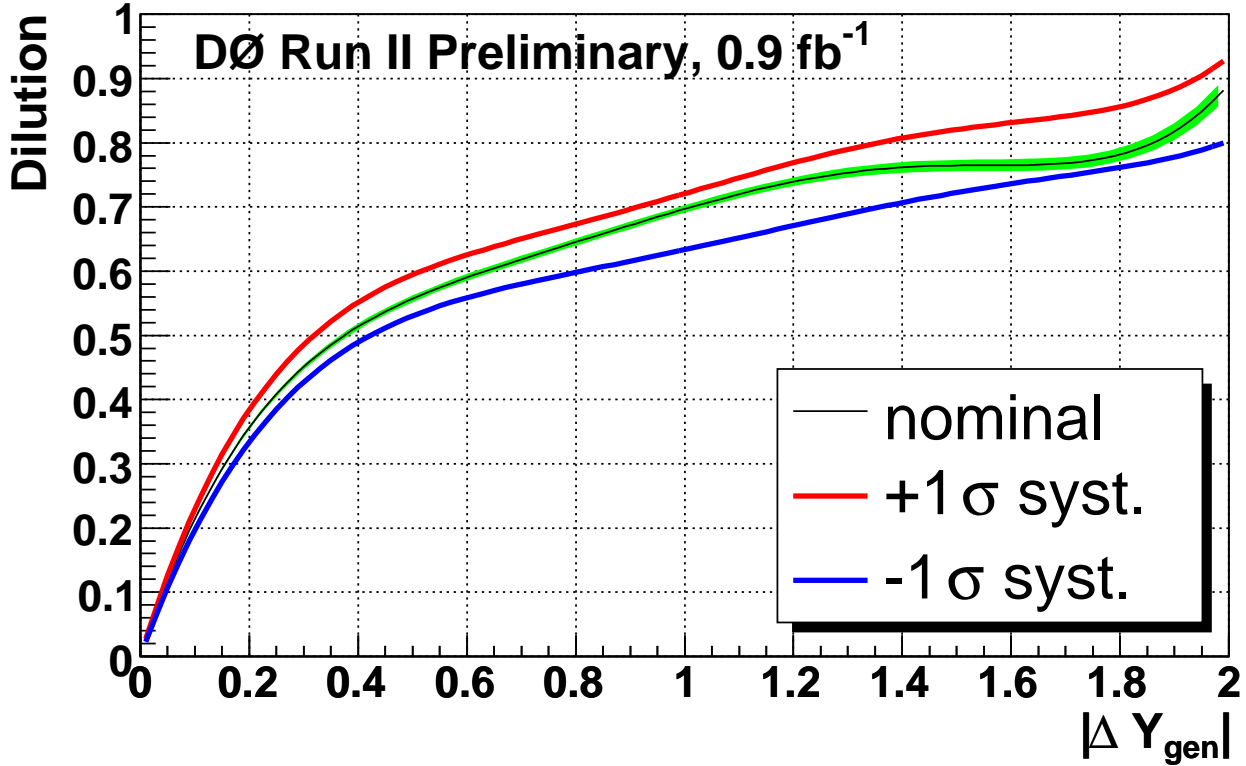


FIG. 2: Geometric dilution as a function of $|\Delta y_{\text{gen}}|$ in fully simulated $t\bar{t}$ events. The plot shows the fit to the nominal dilution (black curve), its fit uncertainties (green band), and the total systematic uncertainties (blue and red curves).

V. DILUTION

Misreconstruction of the sign of Δy dilutes the observed asymmetry. Such dilution can arise from misreconstructing event geometry or from misidentifying lepton charge. The rate of lepton charge misidentification is taken from the signal simulation, and verified using data. It is also possible that misidentification of lepton charge is not forward-backward symmetric, thereby introducing an unwanted asymmetry. Since the polarity of the solenoid magnet is reversed periodically in D0, such effects are below the 1% level for electrons and muons. They are further suppressed in this analysis, as the sign of Δy depends on four additional objects, and thus negligible.

The main dependence of the dilution is on the size of the generated rapidity difference, $|\Delta y_{\text{gen}}|$. The dilution is defined as $\mathcal{D} = 2P - 1$, where P is the probability of reconstructing the correct sign of Δy . It is parametrized as a function of $|\Delta y_{\text{gen}}|$, and estimated (see Fig. 2) from simulated $t\bar{t}$ events generated with PYTHIA [11] and passed through a GEANT-based simulation [12] of the D0 detector. A fit to a polynomial form provides the following analytical expression for the dilution:

$$\mathcal{D}(|\Delta y_{\text{gen}}|) = \sum_{k=1}^5 c_k |\Delta y_{\text{gen}}|^k, \quad (4)$$

with the fit parameters given in Table I.

As this measurement is integrated in $|\Delta y_{\text{gen}}|$, the dilution's strong dependence on $|\Delta y_{\text{gen}}|$ introduces a strong model dependency into any correction from observed A_{fb} to a particle-level A_{fb} . Such a correction factor depends

not only on the model's $|\Delta y_{\text{gen}}|$ distribution, but also on the model's prediction of $A_{fb}(|\Delta y_{\text{gen}}|)$. Furthermore, such a correction can be sensitive to small new physics components of the selected sample. Therefore we present a measurement uncorrected for reconstruction effects, and provide the reader with a parametrization of the dilution that describes these effects, and can be applied to any model.

The dilution also depends somewhat on other variables that affect the quality of $t\bar{t}$ reconstruction, such as the number of jets, primary vertices and b -tags. For variables that are not correlated with asymmetry, any effects are covered by the systematic uncertainties on the dilution. But for variables correlated with asymmetry, the change in reconstruction implies a bias for the observed asymmetry. The largest effect is expected from the number of jets: the reconstruction of the asymmetry in events with five or more jets is inferior to that in four-jet events by 10-25% (relative), depending on $|\Delta y_{\text{gen}}|$. Direct calculations [2] and MC@NLO predict that the asymmetries for the two classes of events differ by 7-13% (absolute). We evaluate the bias using MC@NLO to be $(0.179 \pm 0.015)\%$ (absolute).

VI. ESTIMATION OF BACKGROUND

To estimate the background from W +jets, we define a likelihood discriminant, \mathcal{L} , using variables that are well described in our simulation, provide separation between signal and W +jets background, and do not bias $|\Delta y|$ for the selected signal. The last criterion is specific to this analysis, as many of the common variables used to discriminate between top pairs and W +jets are biased toward central events, and therefore toward small $|\Delta y|$ values that are least suited for measuring the asymmetry. The following set of input variables is used:

- p_T^{lb} - the p_T of the leading b -tagged jet
- χ^2 - of the solution chosen by the constrained kinematic fit to the $t\bar{t}$ hypothesis
- k_T^{min} - defined as $\min(p_T^1, p_T^2) \cdot \Delta R^{12}$, where ΔR^{12} is the angular separation (in η and ϕ) between the two closest jets out of the four jets considered in the kinematic fitter, and p_T^1 and p_T^2 are the transverse momenta of those two jets
- M_{jj} - the invariant mass of the jets the kinematic fitter assigned to the hadronic W decay

After W +jets, the next largest background is from multijet production, where a jet mimics the isolated electron or muon. Following the procedure described in Ref. [7], the normalization of this background is estimated using the large difference between the efficiencies of the lepton criteria for true and false leptons, and the distributions of the likelihood discriminant and the reconstructed asymmetry for this background are taken from samples of data with looser lepton requirements that fail usual lepton criteria. The effects of additional backgrounds which are not considered explicitly when extracting A_{fb} , namely Z +jets, single-top production and di-boson production, are evaluated using ensembles of fake datasets and treated as systematic uncertainties.

VII. ASYMMETRY EXTRACTION

We extract the sample composition and the asymmetry simultaneously using a maximum likelihood fit to the distribution of events. The distribution of the likelihood discriminant and the distribution of $\text{sign}(\Delta y)$ are fitted simultaneously to the sum of four templates: a forward signal template, a backward signal template, a W +jets template, and a multijet template. Both signal templates contain the same likelihood discriminant distribution, and differ only in having all events either forward or backward. The W +jets template contains the simulated reconstructed asymmetry. Though W bosons are generated with an asymmetry of $(22.2 \pm 1.9)\%$, the kinematic reconstruction under the top-pair hypothesis washes out the asymmetry and the reconstructed asymmetry is $(3.0 \pm 1.9)\%$. The signal templates are derived from events generated with PYTHIA, and the W +jets template from events generated with ALPGEN matched with PYTHIA [14]. The multijet template contains an asymmetry from data, corrected for the contribution of other sources (e.g. $t\bar{t}$) in that sample. The fitted parameters are shown in Table II. The fitted correlations between the asymmetry and the other parameters are less than 10%. The fitted asymmetry is $(12 \pm 8)\%$.

VIII. TESTS OF THE METHOD

We test the simulation of production asymmetry, and of the asymmetry reconstructed under the top-pair hypothesis in the W +jets background, by repeating the analysis in a sample enriched in W +jets events. The selection criteria

TABLE II: Sample sizes and fit results. The first line lists the size of the selected data sample, and the second line the size of an auxiliary sample used to derive the multijet background. Lines three to five list the fitted number of events for $t\bar{t}$ signal, W +jets background, and multijet background events in the selected sample. The last line gives the fitted asymmetry. The first column gives the results of the nominal fit. The second and third columns show the results of the same fit procedure done separately for each channel.

	l +jets	e +jets	μ +jets
N_{sel}	379	190	189
N_{aux}	237	162	75
$N^{t\bar{t}}$	264^{+23}_{-22}	127 ± 15	127^{+17}_{-16}
N^W	74 ± 21	34 ± 14	53^{+16}_{-15}
N^{MJ}	41 ± 4	$28.3^{+2.9}_{-2.8}$	$9.7^{+2.3}_{-2.2}$
A_{fb}	$(12 \pm 8) \%$	$(18 \pm 11) \%$	$(9 \pm 12) \%$

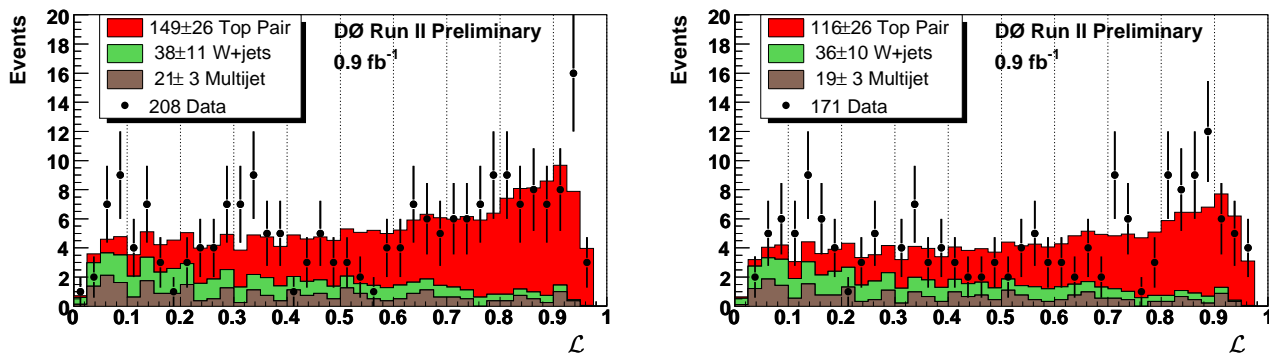


FIG. 3: Comparison of data and its fitted model as a function of the likelihood discriminant for forward events (left) and backward events (right). The number of events from each source is listed in the legend with its statistical uncertainty.

for this sample are identical to the main selection, except that we veto on any b -tags instead of requiring at least one. Both the fully reconstructed asymmetry and the lepton's forward-backward asymmetry are consistent with our model. We also test the fit of the sample composition by deriving a cross section from $N_t^{t\bar{t}}$. This yields a cross section of $7.89^{+0.95}_{-0.93}$ (stat) pb in the e +jets channel, and $8.68^{+1.13}_{-1.11}$ (stat) pb in the μ +jets channel, which are consistent with the dedicated measurements on this data set [13]. We test the fitting procedure, its calibration and its statistical uncertainties using ensembles of pseudodatasets selected from the fit templates. Gaussian statistics are used for the weighted MC templates, and Poisson statistics are used for the data-derived multijet template. A bias of 0.23% is observed and is treated as a systematic uncertainty.

IX. SYSTEMATIC UNCERTAINTIES

The systematic uncertainties on A_{fb} are shown in Table III. The alternative signal model used is ALPGEN matched with PYTHIA [14]. The total uncertainty listed was derived assuming no correlations between various sources. The systematic uncertainties on the jet energy calibration result in possible shifts of the jet thresholds that specify the acceptance. The shifts are $^{+1.3}_{-1.5}$ GeV for the leading jet, and $^{+1.2}_{-1.3}$ GeV for the other jets. The resulting changes in the asymmetry generated by MC@NLO are statistically insignificant and within existing systematic uncertainties. Of the uncertainties listed in Table III, those that effect $t\bar{t}$ signal were considered for the dilution. The total systematic uncertainties on the dilution are shown in Fig. 2, and their parametrization is given above.

X. PRODUCTION VIA A Z' RESONANCE

To demonstrate the measurement's sensitivity to new physics, we study possible $t\bar{t}$ production via a massive electrically neutral gauge bosons, generically referred to as Z' [15]. The $Z' \rightarrow t\bar{t}$ channel is of interest in models with a "leptophobic" Z' that decays dominantly to quarks. We study the scenario where the coupling between the Z' boson and quarks is identical to that between the Z boson and quarks, and interference effects with standard model production are negligible. In particular this assumes predominantly left-handed decays, thus predicting a large positive

TABLE III: Absolute systematic uncertainties on A_{fb} .

Source	σ^+ (in %)	σ^- (in %)
Alternative Signal Model	+0.5	-0.5
Top Quark Mass	+0.3	-0.3
W +jets Heavy Flavor Content	+0.2	-0.2
Jet Efficiencies	+0.0	-0.0
Luminosity	+0.0	-0.0
b -Fragmentation	+0.0	-0.0
Estimation of Multijet Background	+0.1	-0.1
A_{fb} in W +jets Background	+0.5	-0.5
Lepton Charge Misidentification	+0.1	-0.1
Jet Energy Resolution	+0.2	-0.0
Jet Energy Calibration	+0.4	-0.4
b -tagging Rates	+0.5	-0.0
Dilution Bias	+0.2	-0.2
Calibration	+0.2	-0.2
Additional Backgrounds	+0.3	-0.3
MC Template Statistics	+0.1	-0.1
Total	+1.1	-1.0

TABLE IV: Limit setting for production via a Z' resonance. The relative sensitivities are ratios between each sample and the nominal sample. For the selection this is the ratio of selection efficiencies; for the dilution this is a ratio of the average dilutions. The expected and observed 95% C.L. upper limits on the fraction of $t\bar{t}$ events produced via a Z' resonance are shown in the last two columns. Values above one imply no limit.

Z' Mass (in GeV)	Reconstructed Asym. (in %)	Relative Sensitivities		Limits	
		Selection	Dilution	Exp.	Obs.
350 GeV	12.2 ± 1.4	0.82 ± 0.01	0.58 ± 0.16	1.11	1.77
400 GeV	19.7 ± 1.2	0.95 ± 0.01	0.79 ± 0.20	0.70	1.27
450 GeV	19.9 ± 1.1	1.08 ± 0.01	0.90 ± 0.24	0.67	1.30
500 GeV	21.9 ± 1.1	1.17 ± 0.01	1.04 ± 0.27	0.58	1.18
550 GeV	27.6 ± 0.9	1.20 ± 0.01	1.14 ± 0.29	0.44	0.89
600 GeV	25.9 ± 1.0	1.19 ± 0.01	1.21 ± 0.31	0.48	0.96
650 GeV	31.0 ± 1.0	1.13 ± 0.01	1.27 ± 0.33	0.40	0.79
750 GeV	31.1 ± 1.2	0.98 ± 0.01	1.32 ± 0.34	0.44	0.81
850 GeV	33.8 ± 1.2	0.79 ± 0.01	1.34 ± 0.35	0.45	0.78
1000 GeV	37.5 ± 1.5	0.57 ± 0.01	1.32 ± 0.34	0.49	0.77

asymmetry (see Table IV).

Direct searches have ruled out a sizable contribution to $t\bar{t}$ production from a narrow resonance. The top pair asymmetry is sensitive to contributions from both narrow and wide resonances, if their decays are asymmetric. For intermediate Z' masses between 450 and 750 GeV the sensitivity is better than for the $t\bar{t}$ continuum by a factor of up to ≈ 1.4 . Outside that range selection and reconstruction are more difficult and the sensitivity decreases.

We calculate the 95% C.L. upper limit on A_{fb} as its value plus 1.64 times its uncertainty (adding statistical and systematic uncertainties in quadrature), yielding an observed limit of 25.1% and an expected limit of 13.8%.

We translate the limits on the observable asymmetry into limits on the fraction of top pair events produced via a Z' resonance, taking into account the different selection and reconstruction efficiencies, which are taken from fully simulated events generated with PYTHIA. The upper limits described above are translated into the limits listed in Table IV.

XI. CONCLUSIONS

In summary, we present a first measurement of the integrated forward-backward charge asymmetry in top quark pair production. We find that the acceptance shapes the asymmetry and must be specified. We find that corrections for reconstruction effects are too model dependent to be of use. We observe an uncorrected asymmetry of

$$A_{fb}^{obs} = (12 \pm 8 \text{ (stat)} \pm 1 \text{ (syst)}) \% \quad (5)$$

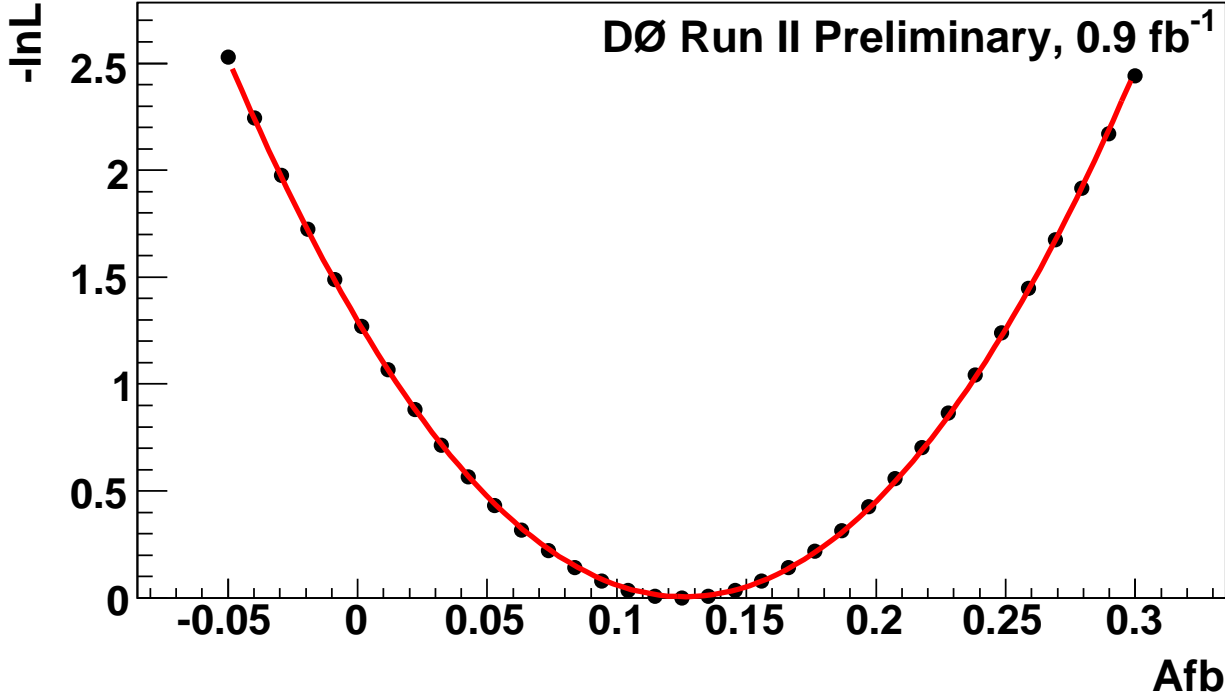


FIG. 4: The maximum likelihood as a function of A_{fb} . The plot shows the fitted minus log likelihood for each fixed A_{fb} value (points) and a second order polynomial fit to the points (curve).

for top-pair events that satisfy the experimental acceptance detailed above, and with the reconstruction dilution detailed above, which can be applied to any model using Eq. 2. The measured asymmetry is consistent with the MC@NLO prediction.

We thank the staffs at Fermilab and collaborating institutions, and acknowledge support from the DOE and NSF (USA); CEA and CNRS/IN2P3 (France); FASI, Rosatom and RFBR (Russia); CAPES, CNPq, FAPERJ, FAPESP and FUNDUNESP (Brazil); DAE and DST (India); Colciencias (Colombia); CONACyT (Mexico); KRF and KOSEF (Korea); CONICET and UBACyT (Argentina); FOM (The Netherlands); Science and Technology Facilities Council (United Kingdom); MSMT and GACR (Czech Republic); CRC Program, CFI, NSERC and WestGrid Project (Canada); BMBF and DFG (Germany); SFI (Ireland); The Swedish Research Council (Sweden); CAS and CNSF (China); Alexander von Humboldt Foundation; and the Marie Curie Program.

-
- [1] J.H. Kühn and G. Rodrigo, Phys. Rev. Lett. **81**, 49 (1998).
 - [2] M.T. Bowen *et al.*, “Standard Model Top Quark Asymmetry at the Fermilab Tevatron”, [hep-ph/0509267] (2006).
 - [3] S. Dittmaier *et al.*, “NLO QCD corrections to $t\bar{t}$ +jet production at hadron colliders”, [hep-ph/0703120, CERN-PH-TH/2007-054] (2007).
 - [4] V. Abazov *et al.* (D0 Collaboration), “The upgraded DØ detector,” Nucl. Instrum. Methods Phys. Res., Sect. A **565**, 463 (2006).
 - [5] S. Frixione and B.R. Webber, “Matching NLO QCD computations and parton shower simulations”, JHEP 0206 (2002) 029 [hep-ph/0204244];
S. Frixione *et al.*, “Matching NLO QCD and parton showers in heavy flavour production”, JHEP 0308 (2003) 007 [hep-ph/0305252].
 - [6] G.C. Blazey *et al.*, in *Proceedings of the Workshop: QCD and Weak Boson Physics in Run II*, edited by U. Baur, R.K. Ellis, and D. Zeppenfeld, Fermilab-Pub-00/297 (2000).
 - [7] V. Abazov *et al.* (D0 Collaboration), “Measurement of the $t\bar{t}$ Production Cross Section in $p\bar{p}$ Collisions at $\sqrt{s} = 1.96$ TeV using Kinematic Characteristics of Lepton + Jets Events”, Phys. Lett. B **626**, 45 (2005).
 - [8] T. Scanlon, Ph.D. thesis, University of London (2006). FERMILAB-THESIS-2006-43.
 - [9] S. Snyder, Doctoral Thesis, State University of New York at Stony Brook (1995).
 - [10] C. Adloff *et al.* (H1 Collaboration), “Measurement of Internal Jet Structure in Dijet Production in Deep-Inelastic Scattering at HERA”, Nucl. Phys. B **545**, 3 (1999).

- [11] T. Sjöstrand *et al.*, Comput. Phys. Commun. **135**, 238 (2001).
- [12] R. Brun and F. Carminati, CERN Program Library Long Writeup W5013, 1993 (unpublished).
- [13] V. Abazov *et al.* (D0 Collaboration), “Measurement of the $t\bar{t}$ Production Cross-Section at $\sqrt{s} = 1.96$ TeV in the Lepton+Jets Final State using a Topological Method on 1 fb^{-1} of D0 Data”, D0 Note 5249-CONF (2006);
V. Abazov *et al.* (D0 Collaboration), “Measurement of the $t\bar{t}$ Production Cross-Section at $\sqrt{s} = 1.96$ TeV in the Lepton+Jets Final State using Neural Network b -tagging algorithm on 1 fb^{-1} of D0 Data”, D0 Note 5335-CONF.
- [14] M. L. Mangano *et al.*, “ALPGEN, a Generator for Hard Multiparton Processes in Hadronic Collisions” [hep-ph/0206293, CERN-TH-2002-129] (2002);
S. Höche *et al.*, “Matching Parton Showers and Matrix Elements”, [hep-ph/0602031].
- [15] W.-M. Yao *et al.*, Journal of Physics G **33**, 1 (2006).

APPENDIX A: ADDITIONAL DETAILS FOR PRESENTERS

This appendix provides additional plots and numbers that presenters may wish to use. A full description of the analysis is in the analysis note.

1. Introduction

- The CDF collaboration presented the outline of a similar analysis at conferences, but has not presented a result (see FERMILAB-THESIS-2006-51).
- Forward events are those where the top quark has a higher rapidity than the antitop quark
- The integrated luminosity is 913 pb^{-1} for the electron channel and 871 pb^{-1} for the muon channel.
- The main background to the signal is from W +jets production. This poses an experimental challenge, as W +jets production has a forward-backward charge asymmetry of $\approx 20\%$.

The prediction for the asymmetry to be observed in this measurement depends on the acceptance and on any dilution arising from misidentification of the charge of the lepton and from mismeasurement of the sign of Δy . The former describes the region of phase space where the asymmetry is measured, and the latter how the observed asymmetry reflects the true asymmetry in that region.

We show that the standard model prediction for the measured asymmetry is $\approx 1\%$, while production through a Z' resonance which couples to quarks similarly to a Z meson yields events that are easily selected and reconstructed in our analysis and have asymmetries of the order of 30%. The large asymmetry difference is used to set limits of the fraction of top pairs produced via such a resonance. This method does not assume a narrow Z' resonance, and is thus complementary to the direct resonance searches.

2. Event Selection and Reconstruction

Selection criteria also include a central primary vertex with at least three tracks, and additional channel-dependent criteria that match the lepton with the PV ($|\Delta z(l, PV)| < 1 \text{ cm}$), veto any overlap between channels, veto $Z \rightarrow \mu\mu$ decays, and match the lepton to the relevant trigger terms. We require that the loose lepton with highest p_T pass the tight selection criteria. Events that fail only this selection make up the loose sample used to study the background from jets that mimic leptons.

To evaluate the benefits of a full reconstruction, we can compare the maximal reconstructible asymmetry, using the MC@NLO prediction for the $|\Delta y_{\text{gen}}|$ distribution within the acceptance, but with 100% asymmetry (the top quark is always forward of the antitop quark). This maximum is $(53.15 \pm 0.07)\%$ for Δy , and $(29.70 \pm 0.07)\%$ for the lepton's charge and direction, a simpler observable suggested in Ref. [2]. As the statistical uncertainties on both observables are the same, this indicates that the kinematic fitter offers an $\approx 80\%$ improvement in the sensitivity to the generated asymmetry.

3. Acceptance

In principle models and data should only be compared within acceptance. Exceptions are very common in top physics,

- mass - all particles of a type have the same mass, so as long as the mass peak is well above the kinematic limit, acceptance plays no role.
- cross section - fixed order calculations are much better at predicting shapes than normalizations, so experimental measurements are corrected for the acceptance according to the theory (MC).

But this is not one of the exceptions. To compare a model to the data, one must calculate the model's predictions within the experimental acceptance. This is why we specify the simple acceptance description.

The correspondence between particle-level jets and reconstructed jets is affected by jet energy calibration, calorimetry resolution, muon corrections, etc. Fortunately, these details can be approximated by simple cuts on particle level jets.

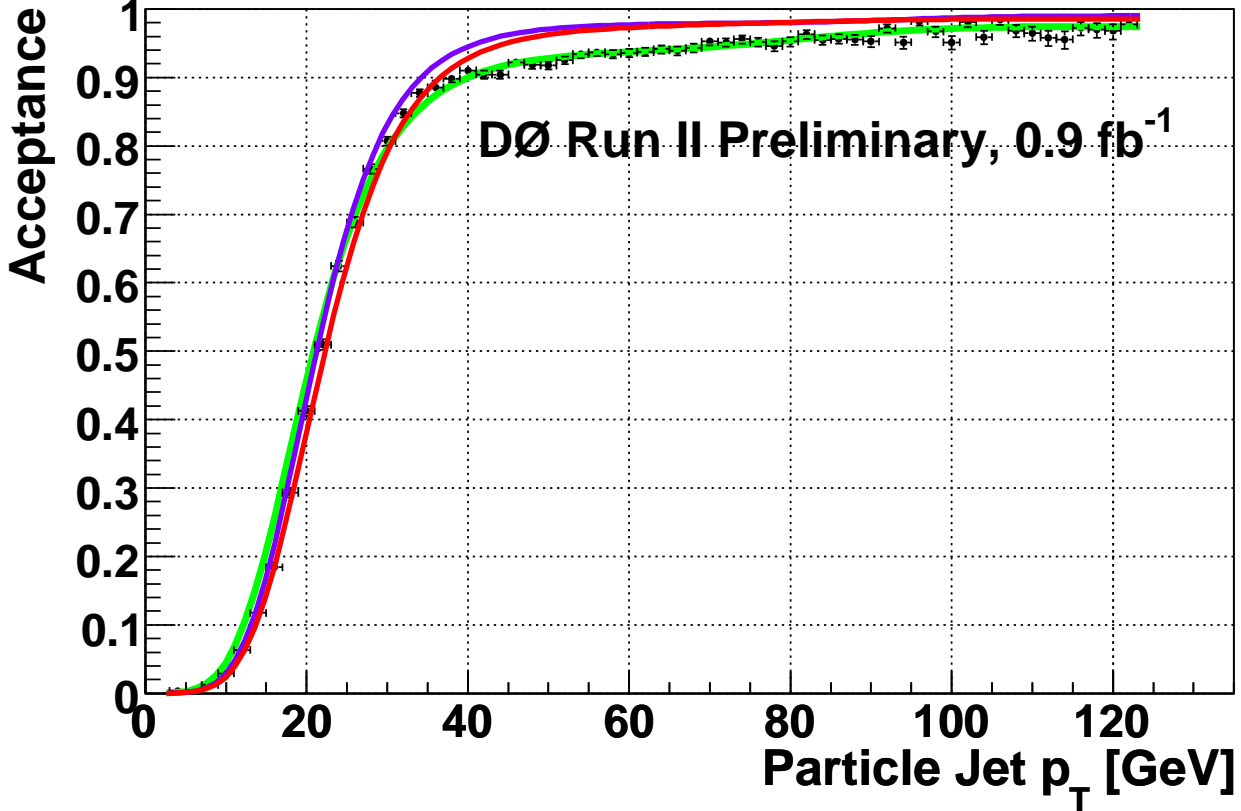


FIG. 5: Jet acceptance by flavor composition, as a function of particle jet p_T . The points show the binned simulated acceptance for the light flavored jets, and the green curve shows the fit to the points. The purple curve shows the fit to the c -jets acceptance, and the red curve shows the fit to the b -jets acceptance.

PXCONE was run so that 50% overlaps trigger split/merge. We’ve verified that PXCONE is stable enough so that the jet reconstruction threshold (p_T) used has a negligible effect. The “E” scheme is also known as the “Run II scheme”.

4. Dilution

This measurement is unusual in that there’s no accurate way to correct the result for reconstruction effects. Instead, when comparing a model to the data, the model’s asymmetry (within the acceptance) must be diluted by the reconstruction effects before comparing to the data result. For this we specify the dilution and its systematic variations.

The $|\Delta y_{\text{gen}}|$ distribution is very roughly a Gaussian with mean 0 and width 1. By definition $A_{fb}(|\Delta y_{\text{gen}}| = 0) = 0$, and A_{fb} is a continuous function of $|\Delta y_{\text{gen}}|$. So the region 0.5-1.0, where the Δy dilution is much better than the lepton-only dilution (see Fig. 10), is important.

5. Estimation of Background

The likelihood discriminant distribution for the additional background sources considered is very close to that for the W +jets background (in fact, for Z +jets it’s statistically consistent). Using ensemble of fake datasets we see that the fitter attributes at least 90% of such events to the W +jets background. To derive this uncertainty we break down the fitted W +jets template yield (71 events) according to the expected sample composition: 44 from W +jets, 18 from Z +jets, 4 from single top production, and 4 from di boson ($WW/WZ/ZZ$) production.

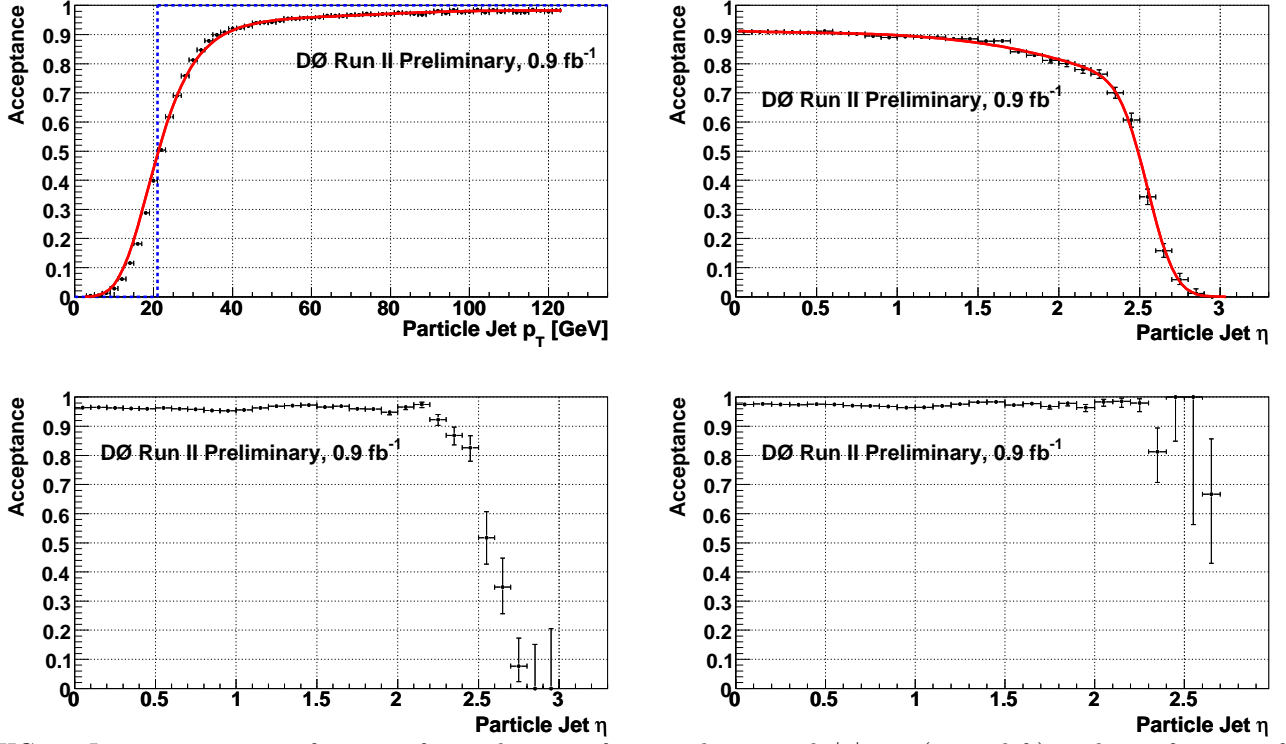


FIG. 6: Jet acceptance as a function of particle-jet p_T for particle jets with $|\eta| < 2$ (upper left), and as a function of η for particle jets with $p_T > 20$ GeV (upper right), $p_T > 40$ GeV (lower left), and $p_T > 60$ GeV (lower right). The points show the binned simulated acceptance, and the solid red curves the fit to the points. The dotted blue curve shows the simple p_T cut. The fits to the upper two plots are used in the analysis.

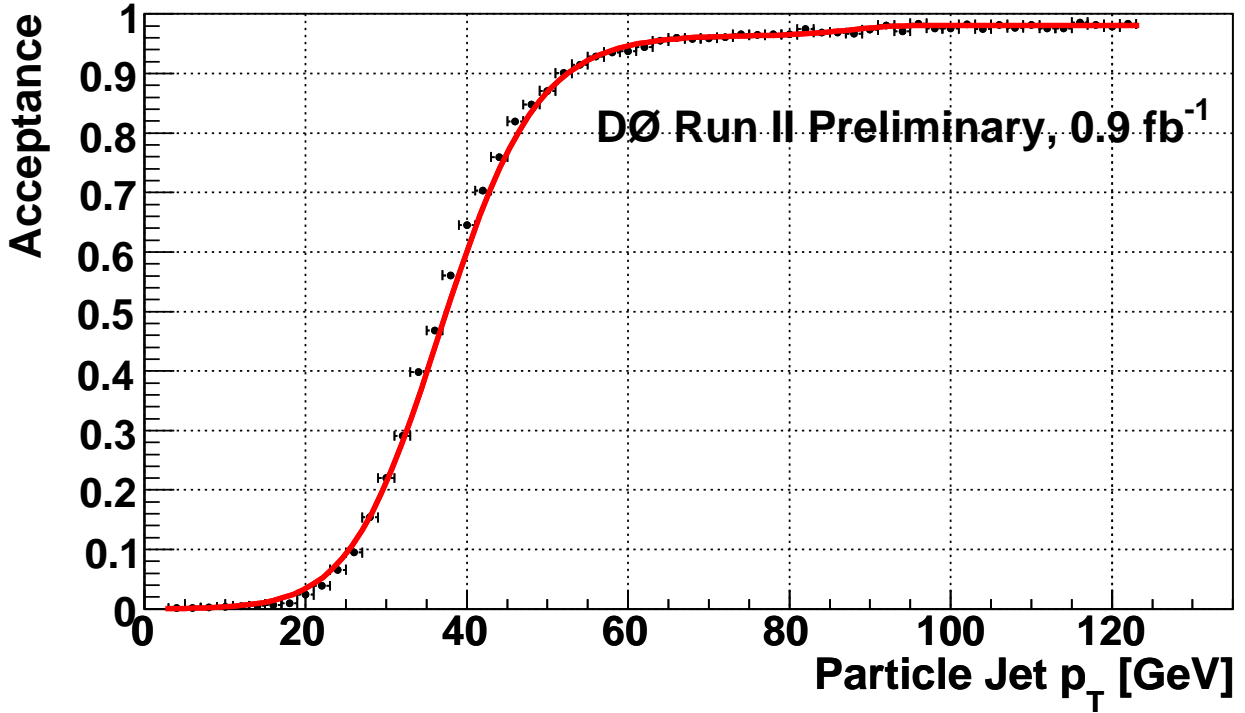


FIG. 7: Jet acceptance including the leading jet criterion $p_T > 35$ GeV, shown as a function of particle jet p_T for particle jets with $|\eta| < 2$. The points show the binned simulated acceptance, and the curves the fit to the points.

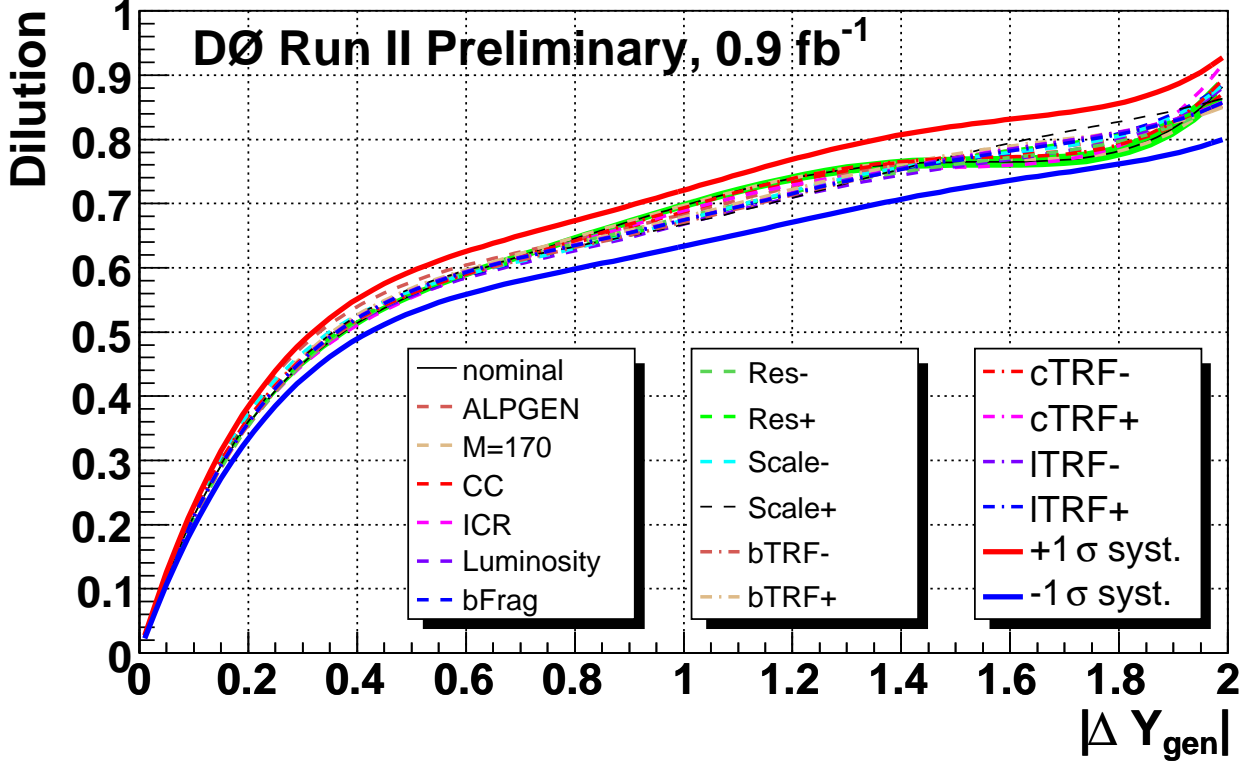


FIG. 8: Geometric dilution as a function of $|\Delta y_{\text{gen}}|$ in fully simulated $t\bar{t}$ events. The curves show fits to nominal (black), its fit uncertainties (green band), and systematically varied dilutions (colored curves). The total systematic uncertainties are represented by the blue and red curves.

6. Asymmetry Extraction

The multijet asymmetry is taken from the loose-tight sample, and is found to be (roughly, because it isn't a fit parameter) $(5 \pm 9)\%$ which is consistent with 0. The uncertainty on the multijet asymmetry due to limited loose-tight statistics is taken from ensembles tests on template statistics that vary it according to Poisson constraints.

The maximal likelihood is:

$$L(N_t^{t\bar{t}}, N_t^W, N_t^{MJ}, A_{fb}) = \left[\prod_i P(n_i^{obs}, \mu_i) \right] \cdot P(N_{l-t}^{obs}, N_{l-t}) \quad (\text{A1})$$

where $N_t^{t\bar{t}}$, N_t^W , and N_t^{MJ} are the fitted numbers of $t\bar{t}$, W +jets, and multijet events in the (tight) sample, respectively, and $P(n, \mu)$ generally denotes the Poisson probability density function for n observed events given an expectation value μ . In the first term of Equation A1, i runs over all the bins of the templates, n_i^{obs} is the content of bin i in selected data, and μ_i is the expectation, which is a function of the fitted parameters:

$$\begin{aligned} \mu_i(N_t^{t\bar{t}}, N_t^W, N_t^{MJ}, A_{fb}) &= N_t^{t\bar{t}} \frac{1 + A_{fb}}{2} f_i^{\Delta y > 0} (1 - C) + N_t^{t\bar{t}} \frac{1 - A_{fb}}{2} f_i^{\Delta y < 0} (1 - C) \\ &+ N_t^W f_i^W (1 - C) + \left(N_t^{MJ} + C(N_t^{t\bar{t}} + N_t^W) \right) f_i^{MJ} \end{aligned} \quad (\text{A2})$$

where $f_i^{\Delta y > 0}$, $f_i^{\Delta y < 0}$, f_i^W , and f_i^{MJ} are the contents of bin i in the following templates, respectively:

- Simulated $t\bar{t}$ signal events with $\Delta y > 0$ (the t quark is reconstructed as more forward than the \bar{t} quark)
- Simulated $t\bar{t}$ signal events with $\Delta y < 0$ (the \bar{t} quark is reconstructed as more forward than the t quark)
- Simulated W +jets events.

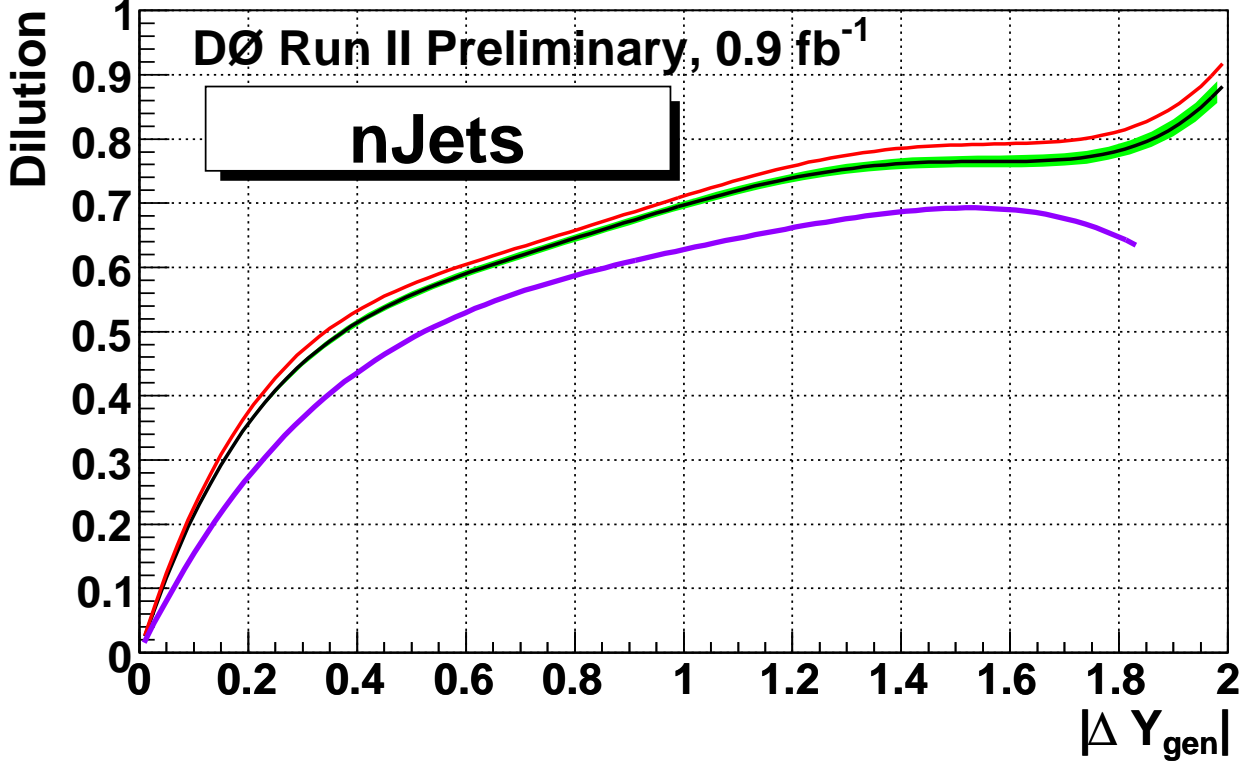


FIG. 9: Geometric dilution as a function of $|\Delta y_{\text{gen}}|$ in simulated $t\bar{t}$ events. The plot shows the nominal fitted dilution (black curve), its fit uncertainties (green band), and the dilutions for events with four jets (red curve) and five or more jets (purple curve).

- The loose-tight data sample, used as a template for multijet background events.

Each template contains the distributions of the likelihood discriminant (\mathcal{L}) and of the sign of the reconstructed Δy , so that the index i in the equations above runs over both distributions. Both signal templates contain the reconstructed Δy , and have the same \mathcal{L} distribution to ensure that the asymmetry is extracted only from the observed Δy . The only difference between them is which of the two $\text{sign}(\Delta y)$ bins is zero and which is one.

The second term of Equation A1 is a Poisson constraint on the observed number of events in the loose-tight data sample N_{l-t}^{obs} and incorporates the Matrix Method in the likelihood. The contamination of loose-tight template by signal and W +jets events is taken into account by using (a detailed derivation is available in D0 Note 5181)

$$N_{l-t} = \frac{1 - \epsilon_{\text{signal}}}{\epsilon_{\text{signal}}} \left(N_t^{t\bar{t}} + N_t^W \right) + \frac{1 - \epsilon_{\text{QCD}}}{\epsilon_{\text{QCD}}} N_t^{MJ} \quad (\text{A3})$$

$$\mathcal{C} = \frac{1 - \epsilon_{\text{signal}}}{\epsilon_{\text{signal}}} \frac{\epsilon_{\text{QCD}}}{1 - \epsilon_{\text{QCD}}} \quad (\text{A4})$$

7. Tests of the Method

The b -tag vetoed sample contains 349 events. We predict that 49% are W +jets, 28% are multijet events, and 23% are $t\bar{t}$. The observed lepton forward-backward asymmetry is $(11 \pm 5)\%$ and is consistent with the expected asymmetry (using MC@NLO for signal), which is $(10.8 \pm 0.8)\%$. The observed $t\bar{t}$ forward-backward asymmetry is $(-1 \pm 5)\%$ and is consistent with the expected asymmetry (using MC@NLO for signal), which is $(3.1 \pm 2.4)\%$.

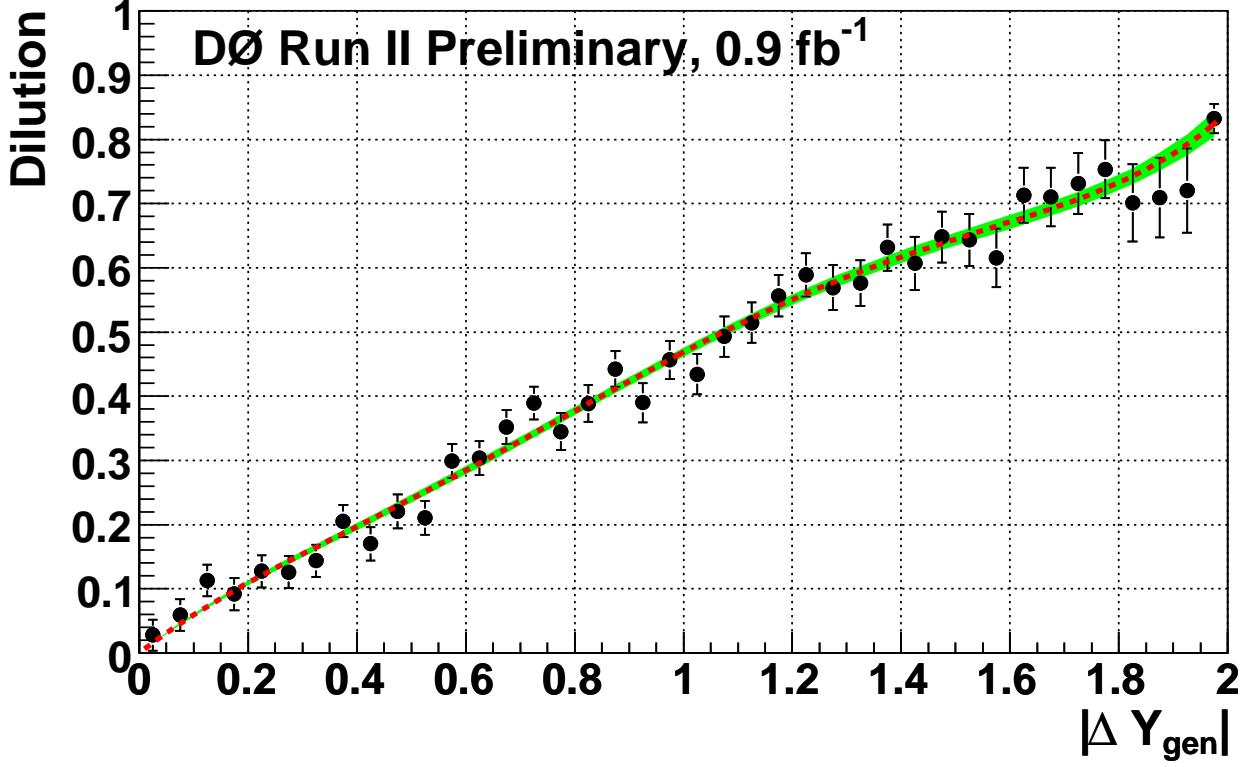


FIG. 10: Geometric dilution for the observable $Q_l \cdot y_l$ as a function of $|\Delta y_{\text{gen}}|$ in simulated $t\bar{t}$ events. The plot shows the results from MC (points), a fit to the points (red curve), and the fit uncertainties (green band).

8. Systematic Uncertainties

A systematic effect such as b-TRFs affecting the asymmetry in W +jets affecting the fitted A_{fb} is listed under $A_{fb}^{W+\text{jets}}$, not under b -tagging.

TABLE V: MC@NLO based predictions of top asymmetry within the experimental acceptance.

N_{jets}	Includes dilution	Asymmetries (in %)	
		Full Acceptance	Simple Acceptance
≥ 4	No	1.1 ± 0.3	1.9 ± 0.3
	Yes	0.8 ± 0.2	1.3 ± 0.2
4	No	3.4 ± 0.4	4.5 ± 0.3
	Yes	2.3 ± 0.2	3.0 ± 0.2
> 4	No	-7.6 ± 0.7	-7.4 ± 0.7
	Yes	-4.9 ± 0.4	-4.9 ± 0.4